

Diamond Cubic Phase of Monoolein and Water as an Amphiphilic Matrix for Electrophoresis of Oligonucleotides

Nils Carlsson,[†] Ann-Sofie Winge,[†] Sven Engström,[‡] and Björn Åkerman^{*,†}

Department of Chemistry and Bioscience and Department of Materials and Surface Chemistry, Chalmers University of Technology, S412 96 Göteborg, Sweden

Received: April 3, 2005; In Final Form: July 21, 2005

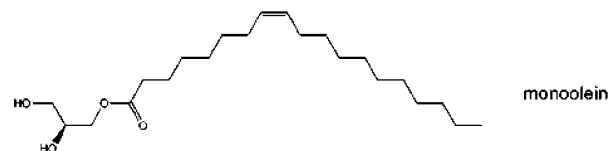
We used a cubic liquid crystal formed by the nonionic monoglyceride monoolein and water as a porous matrix for the electrophoresis of oligonucleotides. The diamond cubic phase is thermodynamically stable when in contact with a water-rich phase, which we exploit to run the electrophoresis in the useful submarine mode. Oligonucleotides are separated according to size and secondary structure by migration through the space-filling aqueous nanometer pores of the regular liquid crystal, but the comparatively slow migration means the cubic phase will not be a replacement for the conventional DNA gels. However, our demonstration that the cubic phase can be used in submarine electrophoresis opens up the possibility for a new matrix for electrophoresis of amphiphilic molecules. From this perspective, the results on the oligonucleotides show that water-soluble particles of nanometer size, typical for the hydrophilic parts of membrane-bound proteins, may be a useful separation motif. A charged contamination in the commercial sample of monoolein, most likely oleic acid that arises from its hydrolysis, restricts useful buffer conditions to a pH below 5.6.

Introduction

The basic mechanism of electrophoretic DNA migration in hydrogels such as agarose and polyacrylamide is well-understood.^{1,2} However, quantitative modeling of the migration is limited to statistical descriptions of the gel structure, because the underlying gelation mechanisms are stochastic in nature, such as phase separation in agarose and free-radical polymerization for polyacrylamide. One approach to obtain more well-defined matrixes for electrophoresis is to use lithography to create obstacle courses of pillars³ or plateaus⁴ sandwiched between two planar surfaces. These structures have been important for improving our understanding of the confined migration of DNA but, to date, have not found major separation applications as a result of their low sample capacity. Another approach is to use amphiphilic lipids or polymers, which together with water self-assemble into lamellar, hexagonal, or cubic phases which often have gel-like properties, albeit being pastier than the solid nature of the conventional hydrogels. These well-ordered liquid crystals contain nanometer aqueous channels confined between micelles or membranes formed by the amphiphile, although they tend to be polycrystalline on macroscopic length scales.

One interesting example is the cubic phase that results from the packing of discrete micelles formed in water by the Pluronic F127 block copolymer of poly(ethylene oxide) and poly(propylene oxide), where the aqueous channels between the micelles are of nanometer dimensions. This structure can be used as a molecular sieve for DNA separation,^{8,9} although larger plasmid-sized DNAs do not enter the pores of the cubic phase but rather migrate along grain boundaries in the polycrystalline structure.^{5,6} The F127 system has a reversed thermal dependence compared to that of agarose in that it forms a flowing solution

CHART 1



at low temperatures (around 10 °C) but turns to the gel-like cubic phase at room temperature.^{7–9} This transformation is reversible, which allows for easy filling and emptying in capillary electrophoresis^{10,11} and for in situ polymerase chain reaction in slab-gel electrophoresis.⁶

A drawback with the phase behavior of the Pluronic system is that its cubic phase cannot be in equilibrium with water. This means that the Pluronic gels tend to dissolve in the parts that are in contact with the buffer chambers that contain the electrodes.⁵ In particular, it is not possible to employ the useful submarine mode of electrophoresis where the gel is covered by buffer to maintain its ionic composition. Here, we try to circumvent this inherent limitation of the Pluronic system by choosing a cubic structure formed by the monoglyceride monoolein (Chart 1) and water.¹² The diamond-type monoolein cubic phase can be in equilibrium with a water-rich phase,^{13,14} which has the potential to act as a buffer reservoir. The first aim of this study was to investigate if the diamond cubic phase can be used in submarine electrophoresis.

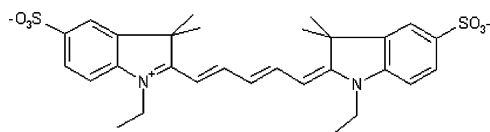
In addition to their well-ordered structure, liquid crystals have an even more interesting advantage over conventional hydrogels in that their amphiphilic nature may allow the analysis of amphiphilic analytes. In this perspective, the monoolein cubic phase differs from the F127 packed micelle type in an important aspect. Monoolein and water form a bicontinuous structure where the lipid bilayer membrane, which lines the space-filling system of aqueous pores, is continuous too, whereas in the F127 micellar cubic phase, the hydrophobic part is discrete. The monoolein cubic phase, thus, allows the transport of membrane-

* Corresponding author.

[†] Department of Chemistry and Bioscience.

[‡] Department of Materials and Surface Chemistry.

CHART 2



bound molecules which is exploited to facilitate the crystallization of membrane proteins, whereas the discontinuous micellar type of cubic phases cannot be used for this purpose.^{15,16} In addition, the monoolein cubic phase has been used to entrap water-soluble proteins in biosensor applications,^{17,18} showing that its hydrophilic channels can act as conduits for the water-soluble enzyme substrates.

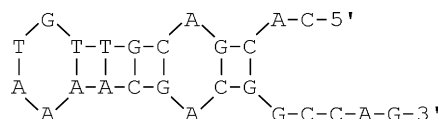
To our knowledge, the monoolein cubic phase has not been used for electrophoretic analysis of either amphiphilic or hydrophilic analytes. We have left the application of this system to membrane-bound molecules to a separate study that focuses on sample transfer into the monoolein membrane (Åkerman et al., submitted), an issue that is particular to such analytes. Here, to avoid this complication, we use water-soluble oligonucleotides to demonstrate that the monoolein cubic phase indeed can be used for submarine electrophoresis. We do not seek to replace the existing agarose and polyacrylamide gels commonly used for DNA; rather, our long-term goal is to use the cubic phase for electrophoretic separation of membrane proteins. Our hypothesis is that successful electrophoretic separation of membrane proteins depends on optimizing both the hydrophilic and the hydrophobic contributions to the total retardation of such membrane-bound analytes. The oligonucleotides used here have hydrodynamic sizes¹⁹ similar to the aqueous pores of the monoolein–water cubic phase¹⁶ and to the hydrophilic parts of the membrane proteins. They are, therefore, suitably sized probes to study the type of friction the hydrophilic parts of the membrane proteins can be expected to experience in the cubic phase and to do so separately from the drag experienced by membrane-anchoring parts, which is being studied separately.

Materials and Methods

Materials. Monoolein was obtained from Danisco and was used without further purification. Metaphor agarose was obtained as a powder from FMC. The following oligonucleotides obtained from SGS DNA, Sweden, will be referred to by the abbreviations as follows: ss25, 3'-GACCGGCAGCAAAAT-GTTGCAGCAC-5'-Cy5; c25, 5'-CTGGCCGTCGTTTTACA-ACGTCGTG-3'; ds25, ss25 + c25; ss12, 3'-TCTCAACTCGTA-5'-Cy5; c12, 5'-AGAGTTGAGCAT-3'; and ds12, ss12 + c12. Cy5 indicates a covalent modification by the fluorescent dye Cy5 (Chart 2), which was used to detect the position and measure the concentration of the oligonucleotide in the gel. Stock concentrations of the oligonucleotides were 13.2 and 16.1 μ M strands for the 25- and 12-base oligomers, respectively, as was determined by the absorbance at 260 nm. The double-stranded samples, ds25 and ds12, were prepared by mixing stoichiometric amounts of strand ss25 (or ss12) and (nonlabeled) the complement strand c25 (or c12).

Unless otherwise stated, all experiments were performed at 20 °C in a 0.2 M acetate buffer ("electrophoresis buffer") and, for gel-stability reasons (described below), at pH 4.0 or 5.6, as is indicated in each experiment. Record²⁰ has shown that calf thymus polynucleotide DNA has a melting temperature of about 45 °C at pH 4 (and about 80 °C at pH 5.6) at an ionic strength of 0.2 M. The melting temperature decreases with decreasing molecular weight, however, so it was deemed necessary to

CHART 3



control the duplex stability for the actual oligonucleotides we used. The fact that the duplex formation was complete and that the double-helical forms were stable against denaturation (strand separation) at pH 5.6 was, therefore, confirmed by electrophoresis in metaphor agarose gels of concentrations between 1 and 5%. Addition of the (nonfluorescent) complement strand gave rise to mobility shifts that showed that the labeled strand was fully engaged in duplex formation.

Notably, the single-stranded oligonucleotide ss25 forms a hairpin structure with six internal base pairs (Chart 3). This was concluded by using the sequence-analysis software Netprimer (available at www.premierbiosoft.com) and confirmed experimentally on high-resolution 5% metaphor gels, where the ss25 unexpectedly migrated faster than the ds25, and the ss12 was slower than ds12, as expected (results not shown). The hairpin secondary structure of ss25 (denoted hp25) also revealed itself by the fact that the hybridization to make the double-stranded 25-mer took several days (presumably because of the slow unpairing of the hairpin), whereas the double-stranded 12-mer formed within minutes. The 12-mer duplex was just barely stable at pH 4, so double-strand experiments were performed at pH 5.6.

Formation of the Cubic Phase as Slab Gels. The diamond-type cubic phase of monoolein is a pastelike phase (here referred to as a gel) that can be in equilibrium with a dilute aqueous solution of the monoolein monomer.^{13,14} The gel was prepared by first melting approximately 10 g of solid monoolein in a water bath at 70 °C. The melt was poured into an electrophoresis tray, kept at room temperature and sealed at the edges, to form an approximately 8-mm-thick layer. The tray was then kept at 8 °C for about 10 h to form a solid white monoolein cake. Finally, this monoolein layer was swollen in the presence of an excess amount of the electrophoresis buffer, provided as an approximately 10-mm-thick layer on top of the monoolein cake. Incubation was performed at 37 °C until the monoolein layer was completely hydrated, as judged by the formation of a fully transparent and isotropic gel that was about 10-mm thick, which took 4–5 days. The hydrated gel usually was uneven in thickness, probably as a result of inhomogeneities that could be seen to exist already in the surface of the solidified monoolein cake before the hydration step. As an evenly thick gel is important for good electrophoresis properties (see below), an even surface was created by shearing off excess paste with a spatula until the gel had a constant thickness. This also improved the optical properties because the inhomogeneities of the original surface reduced the clarity of the gel. Crossed polarizers were used to investigate possible anisotropic structures in the gel.

Gel Electrophoresis and Scanning. Samples contained 0.5–10 μ L of the oligonucleotide stock solution, 4 μ L of a 15% Ficoll solution for loading purposes, and electrophoresis buffer to a total volume of 20 μ L, giving final oligonucleotide concentrations between 0.4 and 8 μ M strands. The conventionally used dye marker bromophenol blue was not used because it tends to associate with amphiphilic matrixes.⁸ Electrophoresis was performed in submarine mode with the horizontal gel covered by electrophoresis buffer. As a result of the need for rather large buffer volumes in the submarine electrophoresis, we used monoolein-free buffer, as opposed to using the equilibrated solution that was obtained in the swelling of the monoolein.

Wells for sample loading were created by pushing a metal spatula (4 mm \times 0.5 mm) once into the monoolein cubic phase with the gel kept under electrophoresis buffer, as this significantly reduced the adhesion between the spatula and the gel. As an alternative approach to sample loading, we also evaluated combination gels with agarose. An agarose solution (1%, 50 °C) was poured around the hydrated monoolein gel, and wells, suitable for accurate sample loading, were formed in the agarose gel by the conventional use of a comb. However, the intended electrophoretic transfer of the oligonucleotide from the agarose to the monoolein often failed because the contact between the two gels was not close and permanent enough, so the sample was often lost in a liquid layer that formed between them. Attempts to have a comb present during the swelling of the monoolein gel were not successful.

We tried to run the electrophoresis in a 50 mM trisborate buffer (pH 8.2) that is conventionally used for DNA. However, in this buffer, the monoolein gel dissolved at the end facing the positive electrode, and extensive foam formation was observed. This was probably a result of an electrophoretic transport of a charged species, possibly an oleic acid contamination that results from the hydrolysis of the (nonionic) monoolein. Attempts to purify the gel from the charged component by pre-electrophoresis (before sample loading) at pH 8 were unsuccessful, because even after 12 h there was still continued dissolution of the gel. With the aim to protonate the oleic acid, we instead used an acetate buffer at pH 5.6 or 4.0. At these pH values, the gel was stable and no foam formation was observed. The current and pH of the buffer was constant for at least 10 h, indicating a stable buffer composition in the gel.

Electrophoresis was run at a constant field strength varied between 2 and 15 V/cm. The field strength in situ in the monoolein gel was measured as the potential difference between a pair of platinum-wire electrodes kept at a distance of 10 mm. It was found that the field strength varied substantially over the gel unless it had been carefully prepared to have an even thickness. The position and intensity of the sample zones were monitored during the continued electrophoresis by repetitive scanning of the gel at regular time intervals. Each scan of the fluorescence distribution on the gel took about 5 min, and the electrophoresis time was corrected for these interruptions. Scanning was performed in a Storm scanner, using a 633-nm excitation of the Cy5 dye and a 650-nm-long pass emission filter. The positions and shapes of the oligonucleotide zones and their integrated intensities were evaluated using the Image Quant software. Control experiments in microtiter plates showed that the integrated intensity from the scanner is proportional to the total amount of dye in the sample, as long as the vertical height (in the direction of the laser light) of the samples is the same. Care was, therefore, taken to load the same total volume of sample in all wells, and when the amount of oligonucleotide was varied, it was accomplished by varying the sample concentration in a given volume.

In the course of the experiments, we found that the integrated fluorescence intensity of the sample zone decreased during the electrophoresis run. Two control experiments were performed to check the possibility that the dye itself or the linker between the dye and the oligonucleotide was unstable as a result of the low pH used in the electrophoresis or resulting from exposure to light. The stability of the dye itself inside the cubic phase was checked by running a sample a few millimeters into the gel by 1 h of electrophoresis, after which the field was turned off. The integrated intensity of the sample zone (while being exposed to pH 4 in the gel) was then measured by fluorescence

scans at regular intervals over a time period of 20 h that was longer than the longest duration of the electrophoresis experiments. This experiment was performed with duplicate samples in different parts of the gel, where one sample was kept in the dark and the other was exposed to the same laboratory-light level as that during the electrophoresis experiments. In a second set of control experiments, several aliquots of the oligonucleotide-dye sample were exposed for different durations to the same electrophoresis buffer (pH 4) but in an Eppendorff tube without monoolein, as a negative control for possible effects from the gel environment on the dye stability. These samples were subsequently analyzed by electrophoresis on a Metaphor agarose gel at pH 7, where the Cy5 is stable.

Fluorescence Spectra in the Buffer and in the Gel. The properties of the Cy5-oligonucleotide samples in the monoolein cubic phase and various solvents were characterized by recording emission spectra using a SPEX fluorimeter. Solution spectra were recorded using an ordinary cuvette. In the monoolein case, the sample was brought a few millimeters into the gel by electrophoresis in the submarine format. The gel was then mounted vertically with the horizontal lightbeam of the fluorimeter entering the front face of the gel and centered in the sample zone. Fluorescence was collected at 90° to the excitation beam through the edge of the gel.

Results and Discussion

1. Nature of the Formed Gel. The protocol of slow swelling of the monoolein in water that we use here is similar to that of the passive-swelling method that is sometimes used to obtain samples for structural studies.¹³ We have not performed any detailed structural studies on the resulting hydrated phase that we use in the electrophoresis experiments, but it was optically transparent and isotropic, as expected for the cubic phase. It is likely that the cubic phase remains during electrophoresis, even if we did not ensure the presence of the (low) monomer concentration in the over-layered buffer, which, strictly speaking, is needed for the equilibrium to be maintained: there was no visible dissolution of the cubic phase over a time period of several days, as long as the pH was 5.6 or lower (see Materials and Methods), and the gel remained transparent and isotropic during electrophoresis.

2. Nature of Oligonucleotide Migration in Monoolein Gels. To our knowledge, the monoolein system has not been used for electrophoresis of biomolecules; therefore, it was important to establish that macromolecules could be transported through the cubic phase. In this first attempt, we used synthetic oligonucleotides to investigate if such monodisperse samples of water-soluble molecules were able to form discrete zones. Figure 1 shows fluorescence images of a monoolein gel recorded after 1 and 8 h (parts a and b of Figure 1, respectively) of electrophoresis of duplicate samples of the Cy-5 modified 12-mer single-stranded oligonucleotide (ss12) at a field strength of 12 V/cm. The wells are indicated at the top of the gel, and distinct zones of the oligonucleotide are seen to have migrated into and through the gel. In this study, we have measured the velocity of migration and investigated if it depends on the size or on other properties of the macromolecules and if the shape and other properties of the zones are suitable for separation applications.

Oligonucleotide Velocity. Figure 2 shows the intensity profile along the left lane in Figure 1 after different durations of the electrophoresis, and Figure 3 shows the derived position of the zone (peak intensity) versus the electrophoresis time for duplicate samples. The plots in Figure 3 are approximately linear

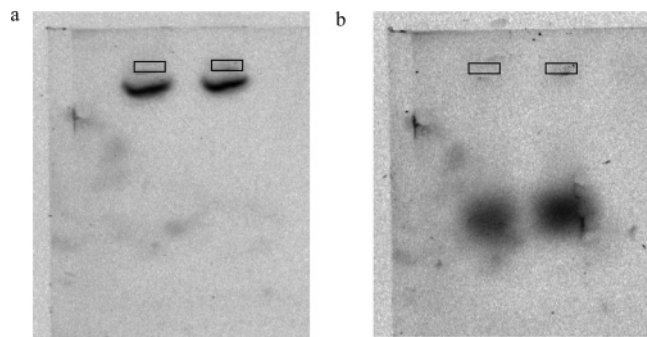


Figure 1. Scan of fluorescence-intensity distribution on a monoolein gel during electrophoresis of duplicate samples of a fluorescein-labeled 12-mer single-stranded oligonucleotide run in separate lanes. The samples (20 μ L of 0.8 μ M strands) were loaded in separate wells (indicated by rectangular boxes), and the gel was scanned after 1 (a) and 8 h (b) of migration at 12 V/cm and 20 $^{\circ}$ C.

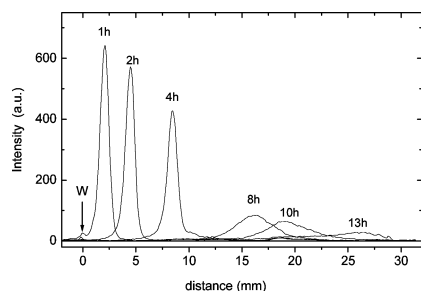


Figure 2. Fluorescence intensity measured along the left lane in Figure 1 after different durations of electrophoresis (indicated). Distance is measured relative to the downfield edge of the well (W).

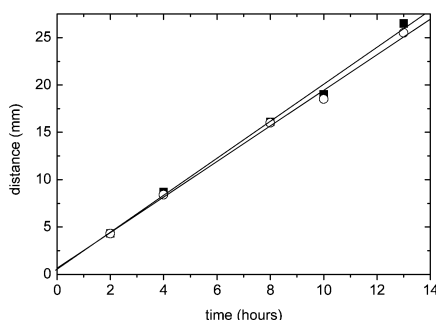


Figure 3. Position of the zone (intensity peak) in Figure 2 (and for the second sample in Figure 1) versus time of electrophoresis. Lines are a least-squares linear fit ($R = 0.998$).

with nearly identical slopes, which shows that the oligonucleotides undergo migration in a reproducible fashion through a matrix that is homogeneous over macroscopic distances. A velocity of 1.94 ± 0.03 mm/h for ss12 can be evaluated from the slopes. This corresponds to an electrophoretic mobility of 4.5×10^{-6} cm² V⁻¹ s⁻¹, which should be compared to the value of about 3×10^{-4} cm² V⁻¹ s⁻¹ in free solution for a double-stranded oligonucleotide of this size²¹ (the single-stranded form can be expected to have 20% lower mobility).²² In fact, the ss12 has a mobility in the cubic phase that is about 4 times smaller than the value 2×10^{-5} cm² V⁻¹ s⁻¹ that is observed for the same oligonucleotide in a 20% polyacrylamide gel (results not shown), the highest concentration that is commonly used in this high-resolution gel. The even lower mobility seen in the cubic phase, which indeed is almost 2 orders of magnitude lower than in free solution, evidences a strong confinement of the oligonucleotide in the monoolein gel. This observation is consistent with migration in channels of molecular dimensions, such as the nanometer-sized pores reported for the cubic phase.¹⁶

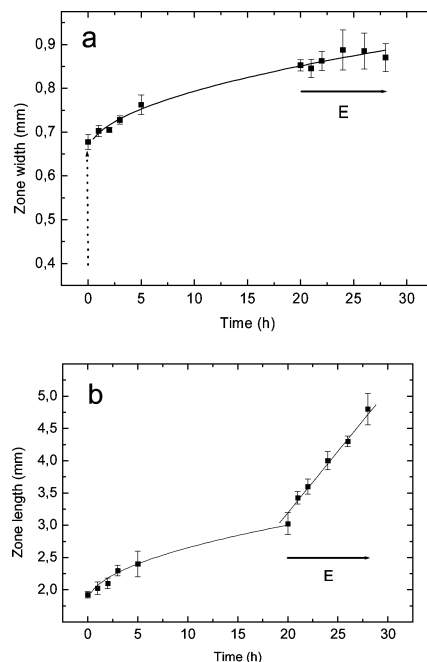


Figure 4. (a) Zone widths perpendicular to the field direction and (b) zone lengths in the direction of the field plotted vs diffusion time (absence of field) between 0 and 20 h and vs electrophoresis time between 20 and 28 h. Curves are least-square fits to $\text{time}^{1/2}$ for 0–28 h in part a and 0–20 h in part b and to time^1 for 20–28 h in part b. Field strength is 12 V/cm. Arrow (E) indicates the presence of an electric field.

By comparison, the diffusion coefficient of water in the cubic monoolein phase is a factor of only about three times lower than that observed in bulk water.²³

We also note that the linear fits pass through the origin, which shows that there is no delay as the oligonucleotides enter the gel. This indicates that there is no severe perturbation at the well–gel interface, such as an increase in gel density due to the mechanical formation of the well.

Shape of the Zones. The velocity results show that oligonucleotides migrate reproducibly in the monoolein gel as well-defined zones that move with a constant velocity. However, as the zone migrates, it becomes longer in the field direction and the peak intensity decreases. This zone lengthening, as well as the width of the zone perpendicular to the field, was measured as a function of time both during migration and in the absence of field.

Figure 4a shows the width of the zones as a function of time, first in the absence of field and then after the field was turned on (horizontal arrow). The fact that the data points in both regimes could be fit to the same square-root dependence supports the suggestion that the lateral widening is caused by diffusion, irrespective of the absence or presence of the electric field. In the absence of field, the length of the zone also increases as the square root of time (Figure 4b), as expected for a diffusional process. However, during electrophoretic migration, the zone length grows significantly faster and, instead, in a linear fashion with time. This shows that the zone extension is not caused by diffusion²⁴ but most likely is a dispersion caused by the migration. This interpretation was supported by experiments at different field strengths (see below).

Integrated Zone Intensity. Figure 2 shows that the peak intensity decreases with time, as expected from the lengthening of the zone. However, closer inspection (Figure 5) reveals that, also, the integrated zone intensity (average of the two samples in Figure 1) decreases with time, by as much as 50% after about

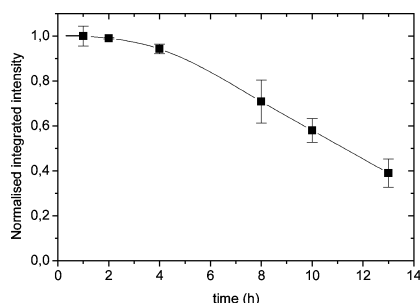


Figure 5. (a) The intensity integrated over the zone vs electrophoresis time. The intensity was integrated in images, such as in Figure 1, over a rectangular area that was large enough to include the whole zone after the longest duration of electrophoresis. Error bars are the difference between duplicate samples. Curve is a guide to the eye.

12 h (or 20 mm) of electrophoresis. The decrease in fluorescence intensity could be due either to a quenching of dye fluorescence in the zone or to a loss of dye from the zone. Self-quenching due to high dye absorbance cannot be the cause of the decreasing intensity because the dye concentration decreases as the zones become longer.

A loss of the oligonucleotide from the zone by adsorption to the membrane walls of the monoolein cubic phase is unlikely. If the lacking integrated intensity between 1 and 13 h was spread as an even smear between the well and the zone position at 13 h, it would result in an average intensity of 20 in the units of Figure 2. This is well above the detected intensity in that region of the gel. Loss of oligonucleotide out of the gel by vertical diffusion is also unlikely because the zone-broadening experiment (Figure 4a) shows that diffusion through the approximately 1-cm-thick gel will be negligible on the time scale of the experiment.

These observations support that the oligonucleotides remain in the zone and that the decrease in intensity is rather a result of a lower emission of the Cy5 dye with time. Even if the intensity decrease is slow, it may be an important effect in analytical applications considering the generally slow migration in the monoolein gel and it was, therefore, investigated in some more detail. The results will be presented after we report our main investigations of zone velocity and shape as a function of the concentration, molecular weight, and secondary structure of the oligonucleotides and the field strength

3. Effect of DNA Concentration in the Zones. First, the oligonucleotide concentration was varied with the aim to optimize electrophoresis conditions regarding zone shape and detection sensitivity. Six different concentrations between 0.4 and 8 μM ss12 strands were loaded in separate wells, and all samples entered the gel as distinct zones (result not shown). As discussed in more detail below, the integrated intensity decreased monotonically with time for all samples (Figure 6a). For the moment, we note that the decrease was approximately monoexponential (Figure 6b), except maybe at the lowest concentration, and from the fits we obtained the integrated intensity at time zero (I_0 ; Figure 7a) and the half-life (Figure 7b) for the decay of the zone intensity. When the I_0 values were plotted versus the loaded concentration, there was a scattered deviation from the expected linear relationship. We ascribe this scattering to the still rather crude protocol for well formation, which may influence the efficiency of the transfer of the sample into the gel, especially at high loadings. The I_0 values were used as estimates of the actual oligonucleotide concentration in the zones after entry from the well. We have not calibrated the fluorescence intensity in terms of absolute concentrations, but for clarity of presentation, the I_0 values were converted into

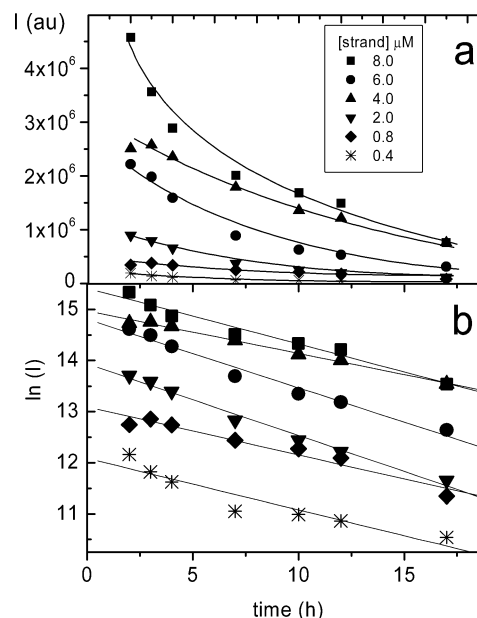


Figure 6. (a) Zone-integrated intensities (obtained as in Figure 5) vs electrophoresis time (at 5.5 V/cm) for different oligonucleotide concentrations (indicated). (b) Semilogarithmic plots of the data in part a. Curves are a least-squares linear fit from which the initial intensity (I_0) and half-life ($t_{1/2} = (\ln 2)/\text{slope}$) for the intensity decrease were evaluated.

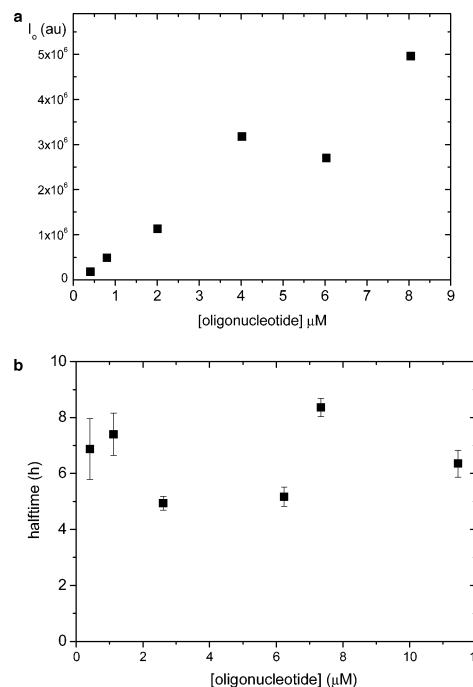


Figure 7. (a) Initial intensity I_0 (from Figure 6) vs the loaded amount of the oligonucleotide (given as strand concentration in the loaded 20 μL of sample). (b) Half-life, $t_{1/2}$, from Figure 6 vs the oligonucleotide concentration in the zone, calculated from I_0 values obtained as described in the text. Error bars are the difference between duplicate samples.

strand concentrations in the zones by assuming that, for the lowest concentration, the entire sample was transferred into the gel. Thus, if anything, the reported oligonucleotide concentrations inside the cubic phase are overestimated.

For all concentrations, the peak position varied linearly with the electrophoresis time, as in Figure 3 (results not shown), and Figure 8 shows that there is no systematic effect of the oligonucleotide concentration on the velocity, as evaluated from

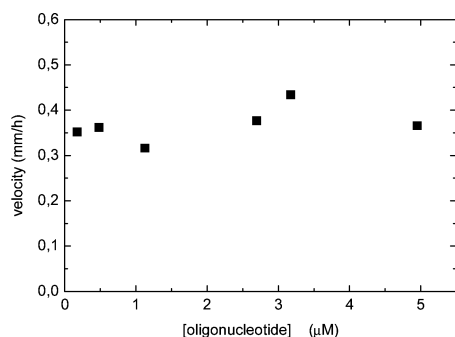


Figure 8. Electrophoretic velocity (obtained from the slopes, as in Figure 3) vs the ss12 oligonucleotide concentration in the zones. Field strength is 5.5 V/cm.

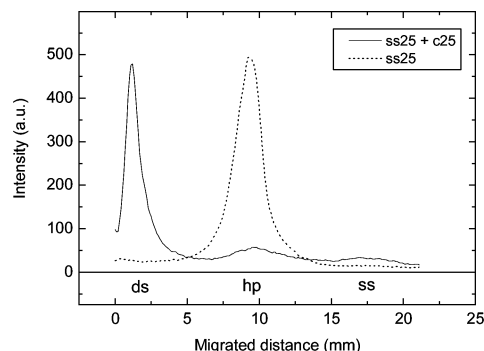


Figure 9. Intensity profiles along the gel after electrophoretic analysis of the ds25 (solid) and ss25 (dotted) samples in the monoolein cubic phase at 5 V/cm. Sample ss25 contains only one component, assigned as 25-mer hairpin (see Materials and Methods). Sample ds25 contains three components, assigned as (in order of increasing velocity) double-stranded 25-mer (ds), hairpin 25-mer (hp), and unfolded single-stranded 25-mer (ss).

the slopes. This is not an unexpected result because even the highest strand concentration we use is below the overlap concentration of the oligonucleotide; thus, strand-strand interactions should be small. If the volume excluded by the lipid material is taken into account (approximately 60%), the average distance between oligonucleotides at a strand concentration of 8 μM is 44 nm, which is 9 times the maximum length of 5 nm for the 12-mer oligonucleotide when fully extended.

4. Mechanism of Electrophoretic Migration and Separation. *Effect of Size and Secondary Structure on the Oligonucleotide Velocity.* The electrophoretic migration of the four oligonucleotides ss12, ds12, ss25, and ds25 was studied at pH 5.6. This pH is low enough to allow the monoolein gel to be stable and still high enough to ensure that the double-helical forms of the oligonucleotides were stable toward strand separation at the present ionic strength and at 20 °C. (see Materials and Methods for details). Figure 9 shows the intensity profile for the ss25 and ds25 samples after 6 h of electrophoresis at 5 V/cm. With ss25, we only observe one zone, which was assigned as the hairpin 25-mer (25hp, see Materials and Methods). In the case of ds25, we observe three components. The major and slowest component was assigned as the double-stranded 25-mer, on the basis of it being the major component when the same sample was run on metaphor agarose gels (results not shown). In addition, there is a small fraction of the hairpin (which is seen comigrating with the single zone in the ss25 sample) and one even weaker and faster component. The latter we tentatively assigned as a small amount of unhybridized 25-mer single strand which had not formed a hairpin, an assignment which is supported by the anomalous field effect we observed for this component (see below). With both the ss12 and the

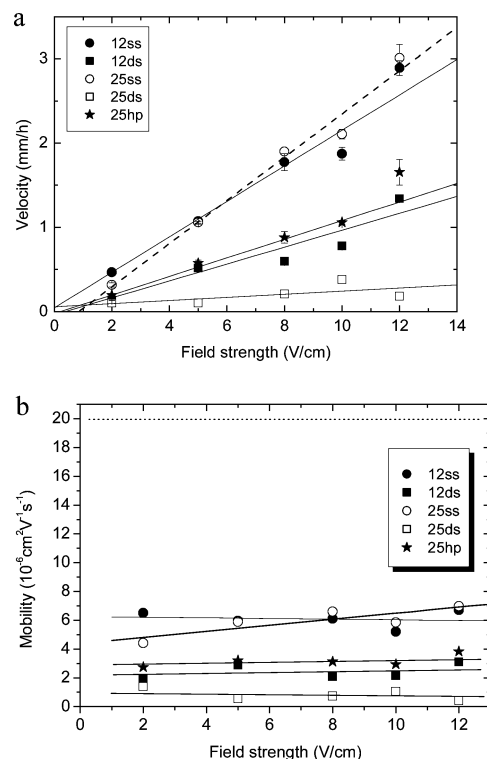


Figure 10. (a) Electrophoretic velocity, v , and (b) mobility, μ , ($\mu = v/E$) vs field strength E for single-stranded (ss) and double-stranded (ds) forms of the 12- and 25-mer oligonucleotides, including a 25-mer hairpin (25 hp; see text). Error bars are the difference between duplicate samples. Dashed line in part b indicates the mobility for the 12-mer ss oligonucleotide in a 20% polyacrylamide gel.

ds12 samples, we observe a single component (not shown) that was assigned as single-stranded and double-stranded 12-mer, respectively.

For all oligonucleotide samples, the migrated distance was linear in time as in Figure 3 (results not shown). Velocities evaluated from the slopes are shown in Figure 10a as a function of field strength. At a given field strength, both the 12- and the 25-mers exhibit lower velocity for the double-stranded form than for the corresponding single strand. In free solution, single-stranded DNA has about 20% lower velocity than the double-stranded form.²² In the monoolein gel, the difference is in the opposite direction and by a factor of about 3 and 6, respectively, for the 12- and 25-mers, so clearly another explanation is needed. The persistence length of double-stranded DNA is 50 nm at the present ionic strength²⁵ and, thus, much longer than the pore diameter (5 nm), whereas single-stranded DNA has a persistence length of about 1 nm.^{26,27} Thus, the strong retardation of the double-helical form suggests that the higher stiffness of the duplex increases the resistance the DNA molecules experience as they negotiate the narrow pores.

Also, for the double-helical form, the velocity decreases with increasing size, because the 12-mer migrates about twice as fast as the 25-mer double strand. This shows that the monoolein cubic phase can separate molecules according to molecular weight. By contrast, the single-stranded forms of the 12- and (nonfolded) 25-mer have approximately the same velocity, an observation we will return to below. In addition, the ss25-mer hairpin is seen to migrate with a velocity similar to that of ds12, consistent with the similar size and shape of a 25-mer hairpin (Chart 3) and a 12-mer duplex. This shows that the electrophoretic velocity also depends on the secondary structure for a given molecular weight. In conclusion, Figure 10a demonstrates that electrophoresis in the monoolein cubic phase is capable of

TABLE 1: Electrophoretic Mobility

oligonucleotide conformation	average mobility ^a (10 ⁻⁶ cm ² V ⁻¹ s ⁻¹)
12-mer single	6.1
12-mer double	2.4
25-mer single	^b
25-mer double	0.83
25-mer hairpin	3.2

^a Average between 2 and 12 V/cm. ^b Mobility is dependent on the field strength (see text).

separating oligonucleotides with respect to molecular size, stiffness, and secondary structure.

Effect of Field Strength on the Oligonucleotide Velocity. Figure 10a also shows that the velocities of the various oligonucleotides increase essentially linearly with the electric field strength. Consequently, the electrophoretic mobilities, $\mu = v/E$, are essentially constant (Figure 10b), and the average values are given in Table 1. The only exception is the nonfolded single-stranded 25-mer, which has a mobility that increases weakly with increasing field strength (an effect which is also seen in Figure 10a because only the ss25-mer has a linear fit that intercepts the ordinate axis at significantly negative velocity values). A nonlinear effect of the field on the electrophoretic velocity usually reveals that the migration causes perturbation of either the macromolecule^{28,29} or the gel structure.⁶ Perturbation of the gel structure tends to give a discontinuous increase in the DNA mobility, as observed at about 12 V/cm for DNA migrating in the cubic phase formed by the amphiphilic copolymer Pluronic F127.⁶ By contrast, in the monoolein cubic phase, the mobility of the 25-mer single strand increases in a continuous fashion (Figure 10b), as is the case in agarose gels where nonlinear field effects are a result of a gradual perturbation of the DNA coils.²⁸ It, therefore, seems more likely that the nonconstant mobility for (nonfolded) ss25 is the result of a perturbation of the DNA conformation rather than of the cubic matrix.

This is further supported by the fact that the nonlinear effect is observed only for one of several different types of DNA molecules. For instance, at a given field strength, the double-stranded form of the 25-mer would be even more likely to perturb the gel. It has a larger charge, is stiffer than the corresponding single-stranded form, and, therefore, can be expected to exert a larger force on the cubic phase structure. Indeed, the higher flexibility of the single-stranded form suggests that its coil would be more prone to becoming deformed than the double-helical molecule, which is expected to behave as a rigid rod. Also, while still being as flexible, the single-stranded 12-mer coil is smaller than the 25-mer coil and, therefore, less likely to have to adapt to the pores. Taken together, these observations could explain why the nonconstant mobility is only observed for the nonfolded 25-mer single strand and, in fact, support this assignment.

Effect of Field Strength on Zone Shape. Figure 11a shows that, after a given time of electrophoresis, the zones are longer as the field becomes stronger, an effect of field that supports the conclusion from Figure 4b that diffusion (which is field-independent) is not the cause of the zone lengthening. Revealingly, the curves of the zone length at the different field strengths merge if they are plotted versus the migrated distance instead of time (Figure 11b), which shows that the zone length is controlled by how far the molecules have traveled rather than by the length of time the molecules have traveled. This observation confirms the proposition made above that zone lengthening in the field direction is caused by a migration-

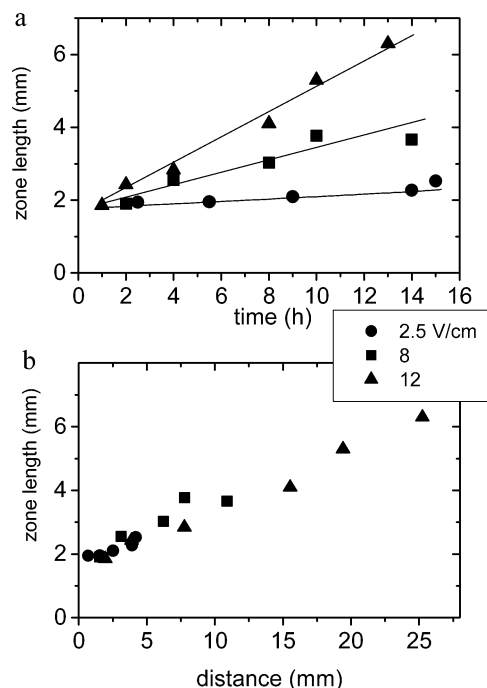


Figure 11. Zone lengths (in the field direction) vs electrophoresis time (top) and vs migrated distance (bottom) during electrophoresis at different field strengths (indicated). Curves are a guide to the eye.

induced dispersion of the molecules resulting from collisions with the monoolein network, as has been observed in conventional gels.²⁴

5. Mechanism of Decrease in Cy5 Fluorescence. Because the loss of the oligonucleotide–dye complex out of the zone cannot explain the decrease in the integrated zone intensity, we performed three experiments to check for the possibility that, rather than the oligonucleotide leaving the zone, the dye is either detached from the oligonucleotide (and leaves the zone) or loses its fluorescence (while still bound to the oligonucleotide in the zone). These possibilities arose in view of the comparatively low pH we use in the monoolein gel in our present protocol. Even though the quantum yield of Cy5 has been reported to be insensitive to pH between 4 and 10,³⁰ the slow migration in the monoolein gel means that the dye is exposed to the acidic environment for unusually long periods of time. For the same reason, there was the possibility that the dye is photobleached as a result of light-exposure during the long electrophoresis runs because Cy5 has been reported to be light sensitive to an extent comparable to fluorescein.³⁰ In addition, we designed these control experiments to account for the possibility that the dye becomes detached from the oligonucleotide, for instance, by hydrolysis of the linker at the acidic pH. Such an effect could explain the loss of fluorescence from the zone because the dye is likely to have a different mobility than the oligonucleotide itself.

Effect of Acidic pH on the Cy5–Oligonucleotide Linkage. In the first experiment, the stability of the dye–oligonucleotide coupling at pH 4 was investigated. Samples of the ss12 oligonucleotide–dye complex were exposed to a pH 4 in monoolein-free test tubes between 0 and 180 min and then were analyzed by agarose-gel electrophoresis at pH 7, where the oligonucleotide–dye complex is stable. The results showed that there is no hydrolysis of the DNA–dye linker (nor of the DNA backbone) because all samples formed a distinct zone with the same velocity as the oligonucleotide in the control sample, which was only exposed to pH 7 (results not shown). Any detached Cy5 dye would have formed a zone between the well and the

oligonucleotide zone because this was the zone position for a reference sample of free fluorescein, which is smaller and has a larger charge (-2) than Cy5 (-1). However, we noted that the integrated intensity of the oligonucleotide zones on the agarose gel decreased with an increasing time of acidic exposure and, furthermore, this loss of fluorescence was less marked when the experiment was performed at pH 5.6 and was virtually absent at pH 7 (results not shown). This observation suggested that, while remaining attached to the oligonucleotide, the Cy5 dye loses its fluorescence by the long-time exposure to low pH.

The possibility of an acidic degradation of Cy5 itself was first investigated in monoolein-free buffer, and, subsequently, the effect of the monoolein cubic phase environment was tested.

Effect of Acidic pH on Cy5 Stability in Free Solution. The decrease in fluorescence intensity in buffer at pH 4 was quantified by spectroscopic fluorescence-intensity measurements in a cuvette, which have smaller sources of error than the gel-scan experiments. Figure 12a shows emission spectra of the Cy5-oligonucleotide complex after different durations of exposure to pH 4. It is seen that the shape of the emission spectrum is retained, but the amplitude decreases in a monotonic fashion with time. The semilogarithmic plot in the inset of Figure 12a gives a half-life of 4.1 h for the decay of the fluorescence intensity at pH 4, whereas at pH 7, the dye was essentially stable (half-life of about 188 h).

Cy5 Stability in the Monoolein Gel. In a second experiment, the stability of the Cy5 dye inside the actual monoolein gel at pH 4 was investigated in the absence and presence of the electric field by the two-step electrophoretic procedure used in Figure 4. Two ss12 samples were introduced into the gel as zones by a 1 h electrophoresis, and then the field was turned off. One sample was kept in the dark, and one was exposed to the same laboratory-light level as in all other experiments; the fluorescence was scanned at regular intervals as the zones remained at the same position on the gel for 20 h. Figure 12b (squares) shows that the integrated intensity decreases in the acidic gel environment with a half-life of 38 ± 6 h and that even if the decay is somewhat slower in the absence of the laboratory-light level (half-life of 49 ± 6 h), photobleaching of the dye is not the major cause of the loss of fluorescence under our conditions.

Interestingly, Figure 12b shows that, when the electrophoresis was resumed, the integrated intensity decreased considerably faster than in the absence of field with a half-life of 13 ± 1 h but still not as fast as in free solution (half-life of 4.1 h; intensity-decay data from Figure 12a included as triangles for comparison).

In summary (Table 2), first, the monoolein-free solution experiments (first two columns) show that there is a degradation of the dye fluorescence at acidic pH. Second, the two gel experiments, in the absence of field, show that there is an effect of light, but it is too small to explain by itself the fluorescence loss during electrophoresis. Third, there is a significant protection of the dye in the gel, because at pH 4, the half-life in the gel (without field) is about 9 ($38/4.1$) times longer than in free solution. Fourth, the protection is less efficient during electrophoresis, because then the half-life is only about 3 ($13/4.1$) times longer than in the free solution at pH 4.

Nature of the Environment of the Cy5 Dye in the Cubic Phase. The fact that the Cy5 dye is protected in the monoolein gel suggests that the dye experiences a different environment than the aqueous buffer. This possibility was investigated by using the sensitivity of the Cy5 emission spectrum to the polarity of the environment reported by Buschmann et al.³¹ Figure 12c

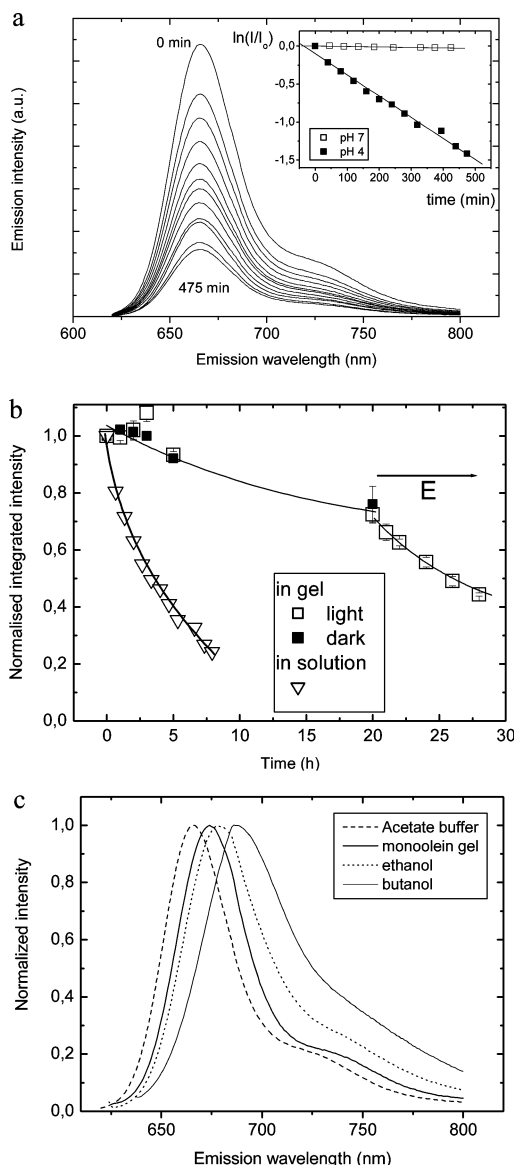


Figure 12. (a). Emission spectra for Cy5-modified oligonucleotides in electrophoresis buffer (no monoolein) after different times of exposure (indicated) at pH 4. Inset shows semilogarithmic plots of integrated intensity vs time at pH 4 and pH 7. Straight lines are a least-squares fit. (b) Integrated zone intensity for Cy5-modified oligonucleotides in the monoolein cubic phase (gel) at pH 4 (rectangles), either in the dark or in normal laboratory light (indicated), and in (monoolein-free) acetate buffer solution at pH 4 (triangles; from part a). Curves are a guide to the eye. The gel experiment was performed as in Figure 4: the field (5 V/cm) was turned off for 20 h after the zone had migrated 2 mm into the gel and was then reapplied, and the zone underwent electrophoresis (E) for 8 h. (c) Emission spectra of the Cy5-modified oligonucleotides in the indicated solvents. Excitation wavelength of 643 nm.

TABLE 2: Half-Life of Cy5 Fluorescence^a

medium condition	solution ^b	solution ^b	gel ^c	gel ^c	gel ^c
pH	4	7	4	4	4
light ^d	yes	yes	no	yes	yes
field ^e	no	no	no	no	yes
half-life (h)	4.1 ± 0.1	188 ± 21	49 ± 6	38 ± 6	13 ± 2

^a Errors in the gel experiments were estimated as standard errors for 2–4 experiments. ^b Obtained by measurements in a cuvette. ^c Obtained by repetitive scanning of the sample zone in the monoolein cubic phase. ^d Laboratory-light level. ^e 5 V/cm.

compares the emission spectra of Cy5 (attached to the ss12 oligonucleotide) in the monoolein gel with those that were

measured in acetate electrophoresis buffer (at pH 4), ethanol, and butanol. It is seen that there is a red shift that is larger as the dielectric constant of the solvent decreases, which is in agreement with the findings by Buschmann et al.³¹ The emission maximum in the monoolein cubic phase is at 674 nm, which is closer to the value in ethanol (679 nm) than to the value in the monoolein-free electrophoresis buffer (666 nm). This indicates that, when inside the gel, the dye is in a less polar environment than water, possibly in contact with the lipid membrane. However, the shift is considerably smaller than expected if the dye were inside the membrane, which has a dielectric constant of about 2.³² The emission properties, thus, suggest that the Cy5 dye is adsorbed to the membrane rather than inserted into it. One possibility is, therefore, that the partially hydrophobic Cy5 adsorbs to the membrane of the cubic structure and that, in this location, it is partially protected from acidic attack.

Effect of Field Strength on the Dye Degradation. The dye degradation in the monoolein gel is three times faster during migration than in the absence of field (Table 2). Importantly, the submarine mode of electrophoresis assured that there were no detectable changes in bulk pH during the 8 h of electrophoresis, so the increased rate is not due to pH changes inside the gel. Furthermore, the decay curves at different fields do not merge when plotted as a function of distance, which indicates that the decay is unrelated to collisions with the gel matrix during migration. We propose that, in the presence of an electric field, the dye is removed from the protective adsorption to the monoolein-membrane environment by being pulled away by the migrating oligonucleotide and is then exposed to the low pH in the pores of the aqueous phase.

Concluding Remarks

The cubic phase formed by monoolein and water is capable of separating oligonucleotides according to size, secondary structure, and flexibility, but the slow migration means that the main interest in the cubic phase is not as a replacement for conventional gels. However, the strong retardation indicates a source of friction that is different in nature from the steric (collisional) one in conventional gels. This conclusion is in accord with the fact that the confining matrix in the cubic phase is a continuous wall, whereas it is a network of discrete fibers in conventional gels. The importance of this distinction is supported by a recent modeling of the migration of water-soluble molecules in the two types of matrixes (Åkerman, in preparation). This unusual nature of retardation in the cubic phase is particularly interesting in view of our long-term goal of the separation of membrane proteins. The similarity in size with the oligonucleotides studied here suggests that the hydrophilic

parts of membrane proteins may be a useful separation motif in the cubic phase, especially now that we have recently shown that membrane-bound analytes indeed can migrate in the cubic phase as well (Åkerman et al., submitted). The restriction to low pH with the present protocol is a problem, as illustrated by the Cy5 degradation, that has to be overcome, for instance, by purification with respect to oleic acid.

References and Notes

- (1) Magnusdottir, S.; Åkerman, B.; Jonsson, M. *J. Phys. Chem.* **1994**, 98, 2624–2633.
- (2) Viovy, J. L. *Rev. Mod. Phys.* **2000**, 72, 813–872.
- (3) Volkmuth, W. D.; Austin, R. H. *Nature* **1992**, 358, 600.
- (4) Han, J.; Craighead, H. G. *Science* **2000**, 288, 1026.
- (5) Svingen, R.; Alexandridis, P.; Åkerman, B. *Langmuir* **2002**, 18, 8616–8619.
- (6) Svingen, R.; Åkerman, B. *J. Phys. Chem. B* **2004**, 108, 2735–2743.
- (7) Wanka, G.; Hoffmann, H.; Ulbricht, W. *Macromolecules* **1994**, 27, 4145–4159.
- (8) Alexandridis, P.; Hatton, T. A. *Colloids Surf., A* **1995**, 96, 1–46.
- (9) Alexandridis, P. *Curr. Opin. Colloid Interface Sci.* **1997**, 2, 478–479.
- (10) Wu, C.; Liu, T.; Chu, B. *Electrophoresis* **1998**, 19, 231–241.
- (11) Rill, R. L.; Locke, B. R.; Liu, Y.; Van Winkle, D. H. *Proc. Natl. Acad. Sci. U.S.A.* **1998**, 95, 1534–1539.
- (12) Larsson, K. *J. Phys. Chem.* **1989**, 93, 7304–7314.
- (13) Briggs, J.; Chung, H.; Caffrey, M. *J. Phys. II* **1996**, 6, 723–751.
- (14) Qiu, H.; Caffrey, M. *Biomaterials* **2000**, 21, 223–234.
- (15) Landau, E. M.; Rosenbusch, J. P. *Proc. Natl. Acad. Sci. U.S.A.* **1996**, 93, 14532–14535.
- (16) Rummel, G.; Hardmeyer, A.; Widmer, C.; Chiu, M. L.; Nollert, P.; Locher, K. P.; Pedruzzi, I.; Landau, E. M.; Rosenbusch, J. P. *J. Struct. Biol.* **1998**, 121, 82–91.
- (17) Razumas, V.; Kanapieniene, J.; Nylander, T.; Engström, S.; Larsson, K. *Anal. Chim. Acta* **1994**, 289, 155–162.
- (18) Barauskas, J.; Razumas, V.; Talaikyte, Z.; Bulovas, A.; Nylander, T.; Tauraitė, D.; Butkus, E. *Chem. Phys. Lipids* **2003**, 123, 87–97.
- (19) Pecora, R. *Science* **1991**, 251, 893–898.
- (20) Record, M. T. *Biopolymers* **1967**, 5, 993–1008.
- (21) Stellwagen, N.; Gelfi, C.; Righetti, P. G. *Biopolymers* **1977**, 42, 687–703.
- (22) Hartford, S. L.; Flygare, W. H. *Macromolecules* **1975**, 8, 80–89.
- (23) Geil, B.; Feiweier, T.; Pospiech, E.-M.; Eisenblätter, J.; Fajara, F.; Winter, R. *Chem. Phys. Lipids* **2000**, 106, 115–126.
- (24) Yarmola, E.; Chrambach, A. *J. Phys. Chem. B* **1998**, 102, 4813.
- (25) Baumann, C. G.; Smith, S. B.; Bloomfield, V. A.; Bustamante, C. *Proc. Natl. Acad. Sci. U.S.A.* **1997**, 94, 6185.
- (26) Tinland, B.; Pluen, A.; Sturm, J.; Weill, G. *Macromolecules* **1997**, 30, 5763.
- (27) Smith, S. B.; Cui, Y.; Bustamante, C. *Science* **1996**, 271, 795–799.
- (28) Åkerman, B. *Electrophoresis* **1996**, 17, 1027–1036.
- (29) Svingen, R.; Takahashi, M.; Åkerman, B. *J. Phys. Chem. B* **2001**, 105, 12879–12893.
- (30) Mujumdar, R. B.; Ernst, L. A.; Mujumdar, S. R.; Lewis, C. J.; Waggoner, A. S. *Bioconjugate Chem.* **1993**, 4, 105–111.
- (31) Buschmann, V.; Weston, K. D.; Sauer, M. *Bioconjugate Chem.* **2003**, 14, 195–204.
- (32) Dilger, J. P.; Benz, R. *J. Membr. Biol.* **1985**, 85, 181–189.